JIPB Journal of Integrative Plant Biology

Research Article
https://doi.org/10.1111/jipb.13830

The MYB61–STRONG2 module regulates culm diameter and lodging resistance in rice

Yong Zhao[1,2,3†], Xianpeng Wang[1†], Jie Gao[1,3,4†], Muhammad Abdul Rehman Rashid[1], Hui Wu[1], Qianfeng Hu[1], Xingming Sun[1], Jinjie Li[1], Hongliang Zhang[1], Peng Xu[5], Qian Qian[4], Chao Chen[6], Zichao Li[1,3,7*] and Zhanying Zhang[1,3*]

1. Frontiers Science Center for Molecular Design Breeding, Key Laboratory of Crop Heterosis and Utilization (MOE), Beijing Key Laboratory of Crop Genetic Improvement, College of Agronomy and Biotechnology, China Agricultural University, Beijing 100193, China
2. Hainan Seed Industry Laboratory, Sanya 572024, China
3. Sanya Institute of China Agricultural University, Sanya 572025, China
4. Yazhouwan National Laboratory, Sanya 572024, China
5. CAS Key Laboratory of Tropical Plant Resources and Sustainable Use, The Xishuangbanna Tropical Botanical Garden, Chinese Academy of Sciences, Menglun 666303, China
6. State Key Laboratory of Crop Germplasm Innovation and Molecular Breeding, Life Science and Technology Center, China National Seed Group Co., Ltd, Wuhan 430073, China
7. Sanya Institute, Hainan Academy of Agricultural Sciences, Sanya 572024, China
†These authors contributed equally to this article.
*Correspondences: Zichao Li (lizichao@cau.edu.cn); Zhanying Zhang (zhangzhanying@cau.edu.cn, Dr. Zhang is fully responsible for the distribution of all materials associated with this article).

Yong Zhao

Zhanying Zhang

ABSTRACT

Lodging reduces grain yield and quality in cereal crops. Lodging resistance is affected by the strength of the culm, which is influenced by the culm diameter, culm wall thickness, and cell wall composition. To explore the genetic architecture of culm diameter in rice (*Oryza sativa*), we conducted a genome-wide association study (GWAS). We identified *STRONG CULM 2* (*STRONG2*), which encodes the mannan synthase CSLA5, and showed that plants that overexpressed this gene had increased culm diameter and improved lodging resistance. *STRONG2* appears to increase the levels of cell wall components, such as mannose and cellulose, thereby enhancing sclerenchyma development in stems. SNP14931253 in the *STRONG2* promoter contributes to variation in *STRONG2* expression in natural germplasms and the transcription factor MYB61 directly activates *STRONG2* expression. Furthermore, *STRONG2* overexpressing plants produced significantly more grains per panicle and heavier grains than the wild-type plants. These results demonstrate that the MYB61–STRONG2 module positively regulates culm diameter and lodging resistance, information that could guide breeding efforts for improved yield in rice.

Keywords: cellulose, CSLA5, lodging resistance, mannose, MYB61, *STRONG2*

Zhao, Y., Wang, X., Gao, J., Rehman Rashid, M. A., Wu, H., Hu, Q., Sun, X., Li, J., Zhang, H., Xu, P., et al. (2025). The MYB61–STRONG2 module regulates culm diameter and lodging resistance in rice. J. Integr. Plant Biol. **67:** 243–257.

INTRODUCTION

Lodging, an important trait limiting rice (*Oryza sativa*) production, is associated with plant height, tiller angle, panicle type, and culm strength. Culm strength is determined by culm diameter, culm wall thickness, and cell wall composition (Kashiwagi et al., 2006; Li et al., 2015).

Plants have primary and secondary cell walls, with primary cell walls providing structure for all cells and secondary cell walls (SCWs) providing mechanical strength for specialized cell types that function in plant growth and water transport. Plant cell walls contain three major polymers: cellulose, hemicellulose, and lignin (Kumar et al., 2016). Cellulose, the most abundant biopolymer on Earth, is biosynthesized by

cellulose synthase (CESA) complexes. Hemicellulose, which is less abundant than cellulose in plant cell walls, is a polysaccharide that includes xyloglucan, xylan, mannan, glucomannan, and mixed-linkage glucan subunits (Scheller and Ulvskov, 2010). Lignin, which is mainly found in SCWs, fills in the cellulose framework, thereby improving the mechanical strength of plants. Cellulose forms crosslinks with hemicellulose and lignin to build a rigid yet flexible structure (Taylor-Teeples et al., 2015).

Hemicellulose biosynthesis in plant cell walls is mainly catalyzed by cellulose-synthase-like (CSL) proteins, including CSLA, CSLB, CSLC, CSLD, CSLE, CSLF, CSLG, CSLH, and CSLJ subfamily members (Yin et al., 2014; Kaur et al., 2017; Zhang et al., 2023). CSLC mediates the biosynthesis of the xyloglucan backbone, and CSLF, CSLH, and CSLJ participate in mixed-linkage glucan biosynthesis (Burton et al., 2006; Cocuron et al., 2007; Doblin et al., 2009; Little et al., 2019). CSLD shares high amino acid similarity with CESA and is involved in the biosynthesis of several glycans (Peng et al., 2019; Yang et al., 2020). CSLA catalyzes the biosynthesis of mannan, which is commonly present in the SCWs of most cell types in Arabidopsis (*Arabidopsis thaliana*) (Handford et al., 2003; Zou et al., 2017). However, the functions of the other subfamily members are not well understood.

To date, only three genes encoding CSLs have been identified in rice. *OsCSLD1* shows root-specific expression and participates in the morphogenesis of root hairs (Kim et al., 2007). *OsCSLD4* (also known as *NARROW AND ROLLED LEAF 1* (*NRL1*), *DWAF AND NARROWED LEAF1* (*DNL1*), and *SLENDER LEAF 1* (*SLE1*)) plays important roles in leaf morphology, plant architecture, and plant responses to salt stress. *CSLD4* mutants have defects in primary cell wall structure and exhibit changes in the abundance of cell wall components, such as cellulose and xylose (Li et al., 2009; Hu et al., 2010; Yoshikawa et al., 2013; Ding et al., 2015; Zhao et al., 2022). The functional deficiency of CSLF6 reduces hemicellulose contents, resulting in a fragile cell wall and reduced mechanical strength (Vega-Sánchez et al., 2012). None of the nine genes encoding CSLAs in rice has been characterized. Given that, it is important to explore the roles of CSLA genes in plant development, especially SCW formation.

Here, using a genome-wide association study (GWAS), we isolated the CSLA-encoding gene *STRONG2*, which positively regulates culm diameter by increasing mannose and cellulose contents in rice. Our results suggest that MYB61 regulates *STRONG2* expression to promote lodging resistance. These findings shed light on the molecular mechanism of lodging resistance and provide insights for improving grain yield via rice breeding.

RESULTS

Identification of *STRONG2* by GWAS

Rice culm diameter is a major factor determining lodging resistance (Okuno et al., 2014). To identify the genes regulating culm diameter in rice germplasm, we selected 141 *japonica* and 199 *indica* rice cultivars for GWAS (Table S1). Phylogenetic analysis demonstrated that the *japonica* and *indica* subpopulations were distinguishable based on genotype, which was supported by the results of principal component analysis (PCA) (Figure S1A, B). The culm diameter of these 340 cultivars at maturity ranged from 3.5 to 7.5 mm, following a nearly normal distribution. On average, the *indica* cultivars had larger culm diameters than the *japonica* cultivars (Figure S1C, D).

We identified 3,097,189 single-nucleotide polymorphisms (SNPs) from the 340 rice cultivars, with a genome-wide linkage disequilibrium (LD) decay of approximately 206 kb (Figure S2). To further analyze the genetics of rice culm diameter, we used the compressed linear mixed (CMLM) model to conduct a GWAS (Figures 1A, S3). Based on a permutation test, the reference threshold of significance-related signaling loci was determined to be P-value < 0.00001 (Figure S4). The GWAS identified 10 significant signal sites related to culm diameter (Table S2).

Among all significant signal sites, *qOD3.2*, a newly identified locus with the strongest signal located in the 14.86–15.14 Mb interval of chromosome 3, attracted our interest. We conducted local LD analysis at this locus and identified a local LD interval in close LD within the 14.86–14.94 Mb interval (Figure 1B, C). In this region, 13 protein-coding genes were annotated in the Rice Genome Annotation Project (http://rice.plantbiology.msu.edu/), but only 10 of these contained significant SNPs, including seven genes for which expression data exist in the RiceXPro database (Table S3). Among these seven genes, the lead SNP (SNP14931253) was located in the promoter of LOC_Os03g26044. This gene showed the highest expression in stems among the seven genes, as revealed by RT-qPCR (Figure S5), suggesting it might be important in stem development. Therefore, we reasoned that LOC_Os03g26044 might be the causal gene for *qOD3.2*, and we named it *STRONG CULM 2* (*STRONG2*).

According to the annotation from the Rice Genome Annotation Project, *STRONG2* encodes a CSLA mannan synthase. Homologous proteins are widely distributed in monocot and dicot plants. The homologs from monocots, such as *Oryza brachyantha*, *Digitaria exilis*, and *Panicum hallii*, share high sequence similarity (Figure S6A). Multiple sequence alignment revealed that the conserved BcsA family domain of STRONG2 in *O. sativa* has high sequence similarity to those of its homologs in *D. exilis* and maize (*Zea mays*), as well as in the dicots Arabidopsis and soybean (*Glycine max*; Figure S6B).

STRONG2 positively regulates lodging resistance

To verify the function of *STRONG2*, we disrupted *STRONG2* in the Nipponbare (Nip) *japonica* background using CRISPR-Cas9 genome editing and obtained two independent homozygous knockout transgenic lines (*STRONG2*-CR1 and *STRONG2*-CR2). *STRONG2*-CR1 harbors a 21-bp deletion resulting in the loss of amino acids 156–162 located in the BcsA family domain, and *STRONG2*-CR2 harbors two single-base insertions that result in a frameshift and premature

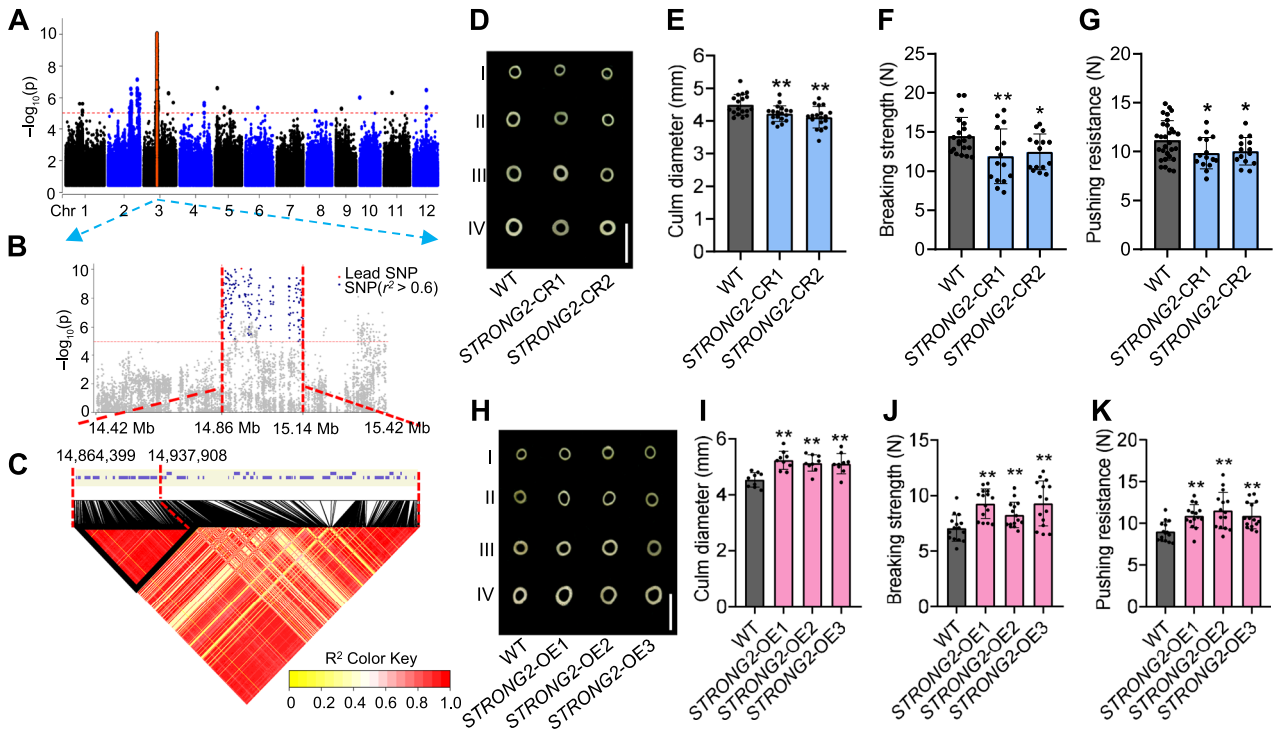

Figure 1. Identification of *STRONG2* by genome-wide association study (GWAS)

(A) Manhattan plot of GWAS for culm diameter. **(B)** Local Manhattan plot for chromosome 3. The red dots indicate lead single-nucleotide polymorphisms (SNP). **(C)** Linkage disequilibrium (LD) plot for SNPs surrounding the peak on chromosome 3. The black triangular block shows the region representing strong local LD ($r^2 \geq 0.6$). **(D)** Culm morphologies of the wild-type (WT) and *STRONG2* knockout lines. Scale bar, 1 cm. **(E–G)** Statistical analysis of the culm diameter **(E)**, breaking strength **(F)**, and pushing resistance **(G)** of the WT and *STRONG2* knockout lines. Values are means ± *SD* ($n > 15$). **(H)** Culm morphologies of the WT and *STRONG2* overexpressing lines. Scale bar, 1 cm. **(I–K)** Statistical analysis of the culm diameter **(I)**, breaking strength **(J)**, and pushing resistance **(K)** in the WT and *STRONG2* overexpressing lines. Values are means ± *SD* ($n > 9$). $^*P < 0.05$; $^{**}P < 0.01$ as determined by two-tailed Student's *t*-test.

termination (Figure S7A, B). Compared with the wild-type (WT), the *STRONG2* knockout lines showed significantly reduced culm diameter, breaking strength (BS), pushing resistance (PR), and section modulus (SM) but no significant difference in culm wall thickness (Figures 1D–G, S7C, D).

To further test the function of *STRONG2*, we generated three homozygous *STRONG2* overexpression lines (*STRONG2*-OE1, *STRONG2*-OE2, and *STRONG2*-OE3) under the control of the CaMV35S promoter (Figure S8A). Compared with the WT, the overexpression lines exhibited increased culm diameter, BS, PR, and SM but similar culm wall thickness (Figures 1H–K, S8B, C). These results demonstrate that *STRONG2* positively regulates culm diameter and thus lodging resistance in rice.

Subcellular localization of STRONG2 and *STRONG2* expression

Subcellular localization of STRONG2 in *Nicotiana tabacum* epidermis cell and rice protoplasts showed that the STRONG2-GFP fusion protein localized to the cytoplasm and plasma membrane (Figure 2A, B). Moreover, we measured the transcript levels of *STRONG2* in different tissues by RT-qPCR. *STRONG2* was expressed in all tissues examined, including leaf blades, leaf sheaths, roots, stems at different stages of development, and panicles (Figure 2C). Finally, we generated a transgenic β-glucuronidase (GUS) reporter line by introducing the *ProSTRONG2:GUS* vector into Nip. *GUS* expression was detected in both the buds and roots of the transgenic plants (Figure 2D [D1]). In mature plants, *GUS* expression was observed in leaf blades, leaf sheaths, roots, stems, and glumes (Figure 2D [D2–D8]). *GUS* was expressed at higher levels in young stems than in mature stems and was highly expressed in vascular bundles and sclerenchyma cells in stems (Figure 2D [D5], E); this pattern is consistent with STRONG2 functioning as a regulator of lodging resistance.

STRONG2 affects SCW formation

CSLA genes contribute to the biosynthesis of SCW components that support culm strength (Handford et al., 2003; Zou et al., 2017). We therefore reasoned that *STRONG2* might affect cell wall structure to regulate lodging resistance. To test this hypothesis, we examined the sclerenchyma in the fourth internodes of WT and *STRONG2* transgenic plants. The sclerenchyma tissue was significantly thicker in the *STRONG2* overexpression lines but thinner in the *STRONG2* knockout lines compared with the WT (Figure 3A, B). Moreover, the large vascular bundles were significantly larger in the *STRONG2* overexpression lines but smaller in the *STRONG2* knockout lines compared with the WT

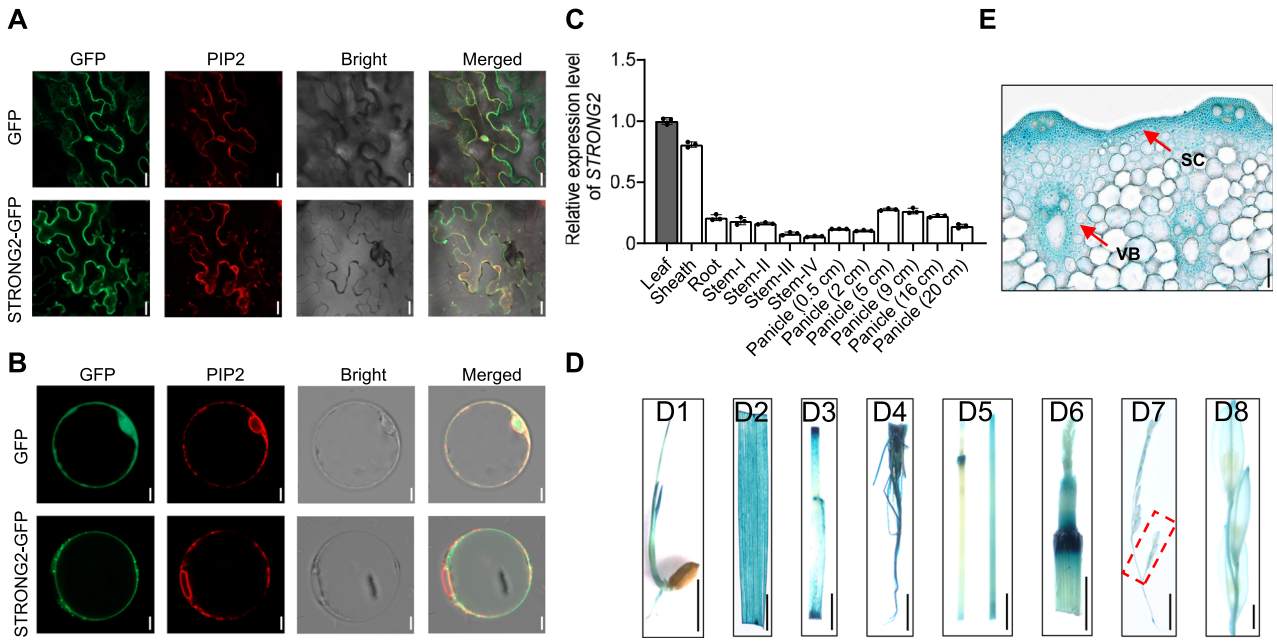

Figure 2. *STRONG2* expression pattern

(A) Subcellular localization of STRONG2 in tobacco. Empty vector pS1300-GFP was the control. Scale bar, 20 μm. **(B)** Subcellular localization of STRONG2 in rice protoplasts. Empty vector pS1300-GFP was the control. Scale bars, 5 μm. **(C)** Expression levels of *STRONG2* in different tissues. Values are means ± *SD* ($n = 3$). **(D)** GUS staining of tissues from *ProSTRONG2*:*GUS* transgenic plants. Seedling (D1), leaf (D2), leaf sheath (D3), root (D4), stem (D5), panicle (D6–D8), Scale bars, 1 cm for (D1–D7); 1 mm for (D8). **(E)** Cross-section of rice stem with GUS staining. SC, sclerenchyma cells; VB, vascular bundle. Scale bar, 1 μm.

(Figure 3C). However, the number of sclerenchyma cell layers and the number of large vascular bundles in the *STRONG2* overexpression and *STRONG2* knockout lines were similar to those in the WT (Figure 3D, E). We also measured sclerenchyma cell wall thickness by scanning electron microscopy. The sclerenchyma cell wall thickness was significantly lower in the *STRONG2* knockout lines but higher in the overexpression lines compared with the WT (Figure 3F, G).

STRONG2 is predicted to encode a mannan synthase, prompting us to measure mannose content in the different lines. The mannose content was lower in the *STRONG2* knockout lines compared with WT, but significantly higher in the overexpression lines (Figure 3H). In addition, we measured the expression levels of several CESA genes, including *OsCESA4*, *OsCESA7*, and *OsCESA9*, by RT-qPCR. These genes were expressed at significantly higher levels in the overexpression lines than in the WT, resulting in higher cellulose contents (Figures 3I, S9A). We examined the relationship between STRONG2 and CESAs in yeast-two-hybrid assays, but did not detect any interactions (Figure S9B). In addition, the lignin content did not differ significantly between the WT and transgenic plants (Figure 3J). Taken together, these findings indicate that *STRONG2* encodes a functioning mannan synthase that plays an important role in SCW formation, thereby regulating culm diameter and culm strength in rice.

Natural variation of *STRONG2* in germplasms

To gain more insight into the natural variation in *STRONG2* among germplasms, we divided the nucleotide sequence of *STRONG2* into five haplotypes (Hap1–Hap5) based on 32 SNPs in the promoter region, coding sequence (CDS), and the 3′ UTR (Figure 4A). There were four haplotypes in the *indica* subpopulation and three haplotypes in the *japonica* subpopulation (Figure 4A). Hap1 existed only in the *japonica* subpopulation, and the culm diameter of these plants was smaller than that of plants harboring Hap2 and Hap4, suggesting that Hap1 is the inferior haplotype (Figure 4B). There were no significant differences in culm diameter among Hap2, Hap3, Hap4, and Hap5 in the *indica* subpopulation or Hap2 and Hap4 in the *japonica* subpopulation (Figure 4C), indicating that the variations in the CDS and the 3′ UTR might not be responsible for the variation in culm diameter. We measured the expression levels of *STRONG2* in different germplasms by RT-qPCR. *STRONG2* was expressed at lower levels in cultivars with Hap1 than in those with the other haplotypes (Hap others; Figure 4D). These results indicate that the variation in culm diameter in different germplasms might be attributed to the variation in the promoter region of *STRONG2*.

To explore whether the SNPs in the promoter regions drove the differences in *STRONG2* expression and culm diameter in these haplotypes, we generated two complementation constructs (*ProSTRONG2*^{Hap1}:*STRONG2*^{Hap1} and *ProSTRONG2*^{Hap4}:*STRONG2*^{Hap1}) and introduced them individually into *STRONG2*-CR1 lines (Figure 4E). *STRONG2* expression was significantly higher in the *ProSTRONG2*^{Hap1}:*STRONG2*^{Hap1} and *ProSTRONG2*^{Hap4}:*STRONG2*^{Hap1} lines compared with *STRONG2*-CR1 (Figure S10A). The culm diameter of *ProSTRONG2*^{Hap4}:*STRONG2*^{Hap1} was significantly greater than that

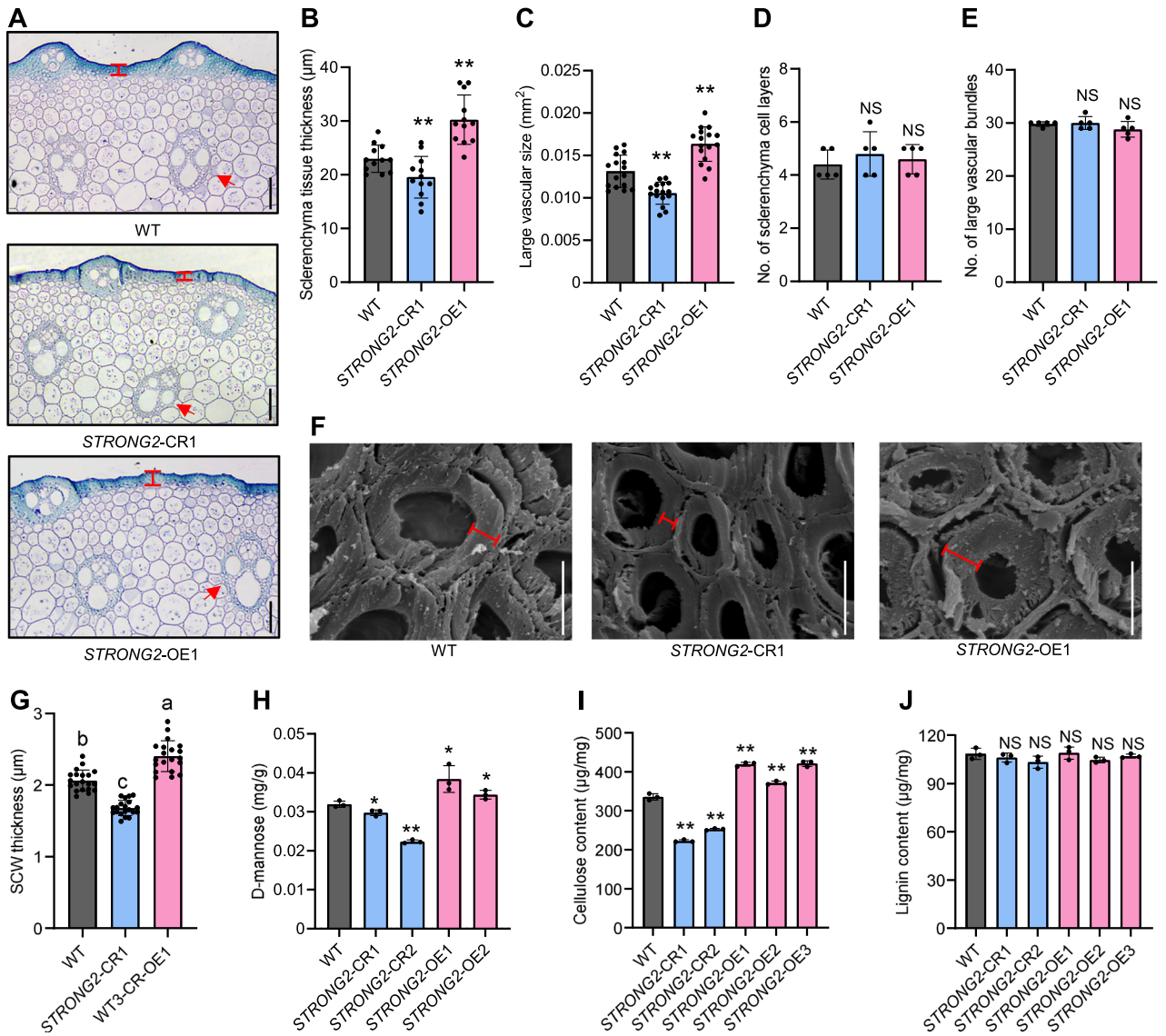

Figure 3. *STRONG2* affects secondary wall formation

(A) The cross-sections stained with toluidine blue of the fourth internodes in wild-type (WT) and *STRONG2* transgenic lines. Scale bars, 100 μm. **(B–E)** Comparison of sclerenchyma tissue thickness **(B)**, large vascular size **(C)**, number of sclerenchyma cell layers **(D)**, and number of large vascular bundles **(E)** of WT and *STRONG2* transgenic lines. Values are means ± *SD*. ($n > 5$). **(F)** Scanning electron microscopy micrographs of sclerenchyma cells from the fourth internodes of the indicated plants. Scale bars, 5 μm. **(G)** Comparison of sclerenchyma cell wall thickness of WT and *STRONG2* transgenic lines. Values are means ± *SD* ($n = 20$). **(H–J)** Mannose **(H)**, cellulose **(I)**, and lignin **(J)** contents in the fourth internodes of WT and *STRONG2* transgenic lines at the mature stage. Values are means ± *SD* ($n = 3$). $^*P < 0.05$; $^{**}P < 0.01$; NS, no significant difference as determined by two-tailed Student's *t*-test.

of *ProSTRONG2*^{Hap1}:*STRONG2*^{Hap1} and *STRONG2*-CR1 (Figure 4F, G). The culm wall thickness did not significantly differ among lines (Figure S10B). These results suggest that *STRONG2*^{Hap4} might be the superior allele and that natural variation in the promoter of *STRONG2* plays an important role in regulating culm diameter in rice.

To explore the origin and evolution of *STRONG2*, we analyzed *STRONG2* sequence variations in 558 cultivated rice accessions and 143 common wild rice (*Oryza rufipogon*) accessions (Table S1). Phylogenetic and haplotype network analysis revealed that Hap1 mainly existed in temperate *japonica* (*tej*) and the wild rice *Or*-III, and other haplotypes mainly existed in *indica* and the wild rice *Or*-I and *Or*-II, indicating that Hap1 might be derived directly from wild rice (Figures 4H, S11). To investigate whether *STRONG2* has undergone selection during rice domestication, we analyzed the nucleotide diversity (π) and Tajima's *D* values of *STRONG2* and its upstream or downstream regions in different subgroups. The π values of *STRONG2* and its flanking regions were significantly lower in *tej* than in the *indica* and tropical *japonica* (*trj*) subpopulations, and the Tajima's *D* values of *STRONG2* and its downstream 20-kb region were negative and deviated significantly from zero (Figure 4I; Table S4), indicating that this gene may have been under positive

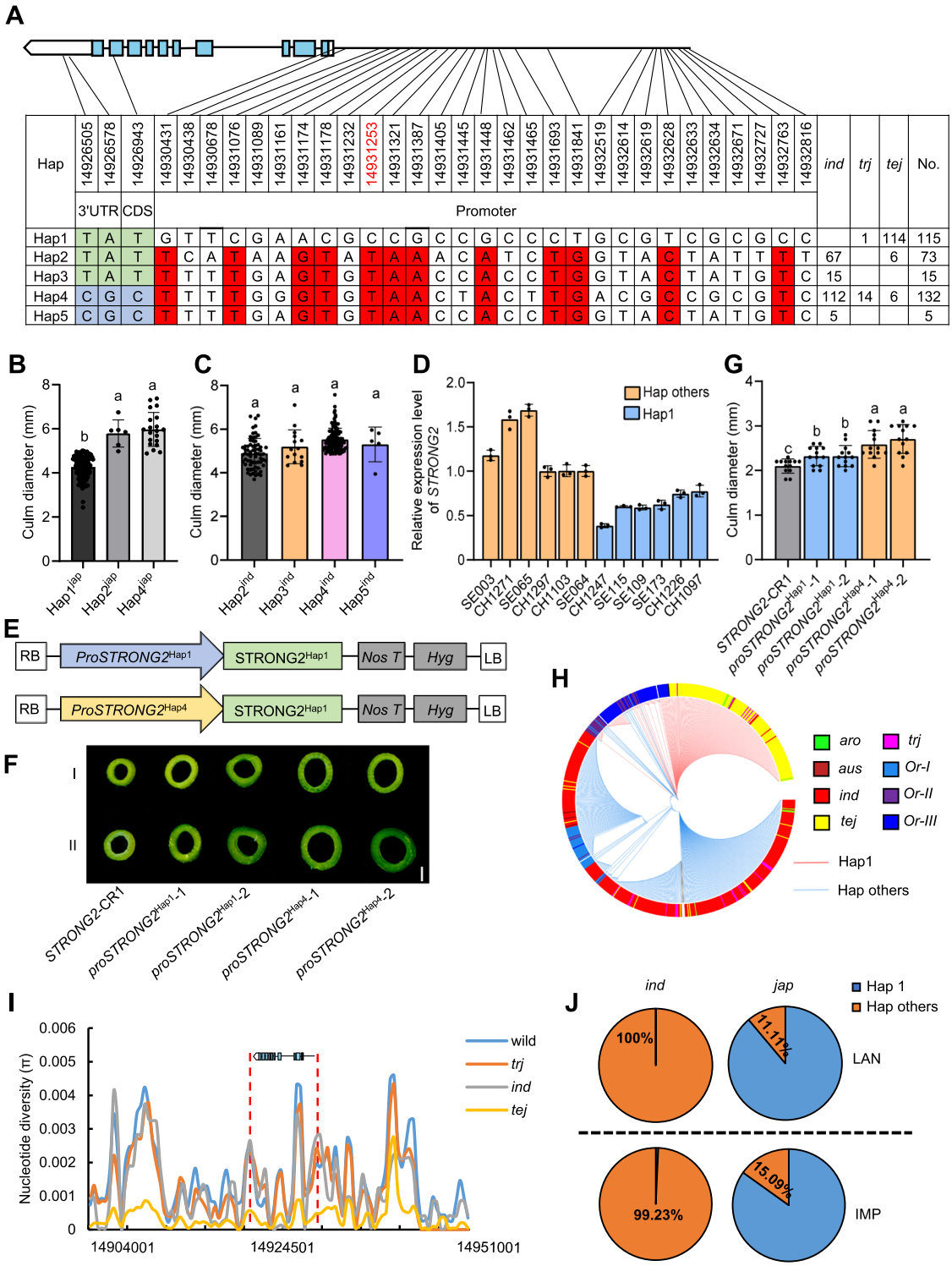

Figure 4. Haplotype analysis and phylogenetic origins of *STRONG2*

(A) Haplotype analysis of *STRONG2* in different subpopulations. The gene structure of *STRONG2* is shown above. *ind*, indica; *trj*, tropical *japonica*; *tej*, temperate *japonica*. **(B, C)** Statistical results for culm diameter in the *jap* **(B)** and *ind* **(C)** subgroup. Values are mean ± *SD* ($n > 5$). **(D)** The relative expression level of *STRONG2* between Hap others and Hap1 in the stem of representative rice varieties. Values are means ± *SD* ($n = 3$). **(E)** Schematic diagrams of complementation vectors. **(F, G)** Culm morphologies and statistical analysis of the second culm diameter of the *STRONG2-CR1* and two complementation lines. Scale bar for **(F)**, 1 mm. Values are means ± *SD* ($n = 13$). **(H)** Phylogenetic tree of *STRONG2*. The color of the outer circle indicates different groups; the color of the inner branch indicates different haps. **(I)** Nucleotide diversity of *STRONG2* in wild rice and cultivated rice. The *x*-axis and *y*-axis indicate the position of *STRONG2* and the average π value, respectively. **(J)** Frequencies of haplotypes in landrace (LAN) and improved (IMP) accessions within the *ind* and *jap* subpopulations. In **(B)**, **(C)** and **(G)**, different lowercase letters indicate a significant difference ($P < 0.05$) based on one-way analysis of variance (ANOVA) with the Duncan test.

selection in *tej*. Moreover, we analyzed the frequency of the Hap1 and Hap others alleles in landraces and improved varieties and determined that the elite alleles (Hap others) have been widely used in *indica*, indicating that these alleles have a strong potential for application in the genetic improvement of lodging resistance in *japonica* rice (Figure 4J).

The MYB61–STRONG2 module regulates culm diameter

To identify the regulator of *STRONG2*, we analyzed the promoter sequence of this gene. We detected binding motifs for several types of transcription factor, including AP2, MYB, NAC, and TCP (Table S5). SNP14931253 (the lead SNP) is located in a MYB binding site. *MYB61* positively regulates SCW thickness and culm diameter (Gao et al., 2020). To test whether *MYB61* affects culm diameter, we generated three *MYB61* knockout lines by CRISPR-Cas9 genome editing, and named them *MYB61*-KO1, *MYB61*-KO2, and *MYB61*-KO3. These lines showed decreased culm diameter (Figure S12A–C). We also generated three *MYB61* overexpression lines, *MYB61*-OE1, *MYB61*-OE2, and *MYB61*-OE3, which had increased culm diameter (Figure S12D–F). Therefore, we reasoned that MYB61 might directly regulate *STRONG2* expression. Indeed, RT-qPCR analysis showed that MYB61 positively regulates *STRONG2* expression in the stem (Figure 5A, B).

We examined the interaction of MYB61 with variants of the *STRONG2* promoter carrying different alleles (C or T) of SNP14931253 using a yeast-one-hybrid assay. MYB61 is directly bound to the promoters of $STRONG2^{14931253C}$ and $STRONG2^{14931253T}$ (Figure 5C). We then co-transfected rice protoplasts with the effector *Pro35S:MYB61* and reporters containing the *STRONG2* promoter driving luciferase expression, including $ProSTRONG2^{14931253C}$*:LUC* and $ProSTRONG2^{14931253T}$*:LUC*. Luciferase activity was higher in $ProSTRONG2^{14931253T}$*:LUC* than in $ProSTRONG2^{14931253C}$*:LUC* (Figure 5D). In addition, luciferase activity was higher in $ProSTRONG2^{14931253T}$*:LUC* than in $ProSTRONG2^{14931253C}$*:LUC* when these constructs were co-expressed with *Pro35S:MYB61* (Figure 5D).

We also conducted chromatin immunoprecipitation (ChIP) assays to explore whether MYB61 binds to the two *STRONG2* promoters *in vivo*. ChIP–qPCR showed high fold enrichment for $ProSTRONG2^{14931253T}$ compared with $ProSTRONG2^{14931253C}$ in the P3 segment containing SNP14931253 (Figure 5E). We performed electrophoretic mobility shift assays (EMSAs) using the P3 segment and confirmed that MYB61-MBP directly binds to the P3 region. This specific binding was inhibited by non-biotin-labeled competitive probes but not by the non-biotin-labeled mutated probes (Figure 5F). In addition, MYB61 showed a stronger binding affinity to the $ProSTRONG2^{14931253T}$ probe than to the $ProSTRONG2^{14931253C}$ probe (Figure 5F). These results demonstrate that MYB61 binds to the promoter region of *STRONG2* both *in vivo* and *in vitro*.

Subsequently, we generated *STRONG2-CR/MYB61-OE* plants by crossing to explore the genetic relationship between *STRONG2* and *MYB61*. The culm diameter of the *STRONG2-CR/MYB61-OE* plants was similar to that of the *STRONG2* knockout lines, indicating that *STRONG2* acts genetically downstream of MYB61 (Figure 5G–I). Taken together, these findings indicate that the MYB61–STRONG2 module positively regulates culm diameter.

Overexpressing *STRONG2* enhances grain yield

To evaluate the breeding value of *STRONG2*, we analyzed its effects on other important agronomic traits. Compared with the WT, *STRONG2* overexpression lines had a similar plant height and panicle length but significantly increased panicle number, primary branch number per panicle (except for *STRONG2*-OE2), secondary branch number per panicle, and grain number per panicle (Figures 6A–E, S13). The grain width of the overexpression lines was similar to that of the WT, but the grain length and 1000-grain weight were significantly increased in the overexpression lines (Figure 6F, G). The grain yield per plant of the *STRONG2*-OE1 and *STRONG2*-OE2 lines was approximately 12.93% and 15.35% higher, respectively, than that of the WT (Figure 6H). By contrast, the *STRONG2* knockout lines showed significantly reduced plant height, panicle length, secondary branch number per panicle, and grain length and thus reductions in grain number per panicle and 1,000-grain weight in the field. However, these lines showed no significant differences in primary branch number per panicle or grain width compared with the WT (Figure S14A–L). The grain yield of the *STRONG2* knockout lines was decreased by approximately 35.94% and 25.30%, respectively (Figure S14M). Furthermore, there were no significant differences in the seed quality of the *STRONG2* knockout or overexpression lines compared with the WT (Figure S15). Taken together, these results demonstrate that overexpressing *STRONG2* can enhance grain yield without affecting seed quality, providing a genetic resource for breeding for increased yield.

DISCUSSION

Lodging reduces the yield and quality of rice and affects the mechanized harvesting of this crop. A strong culm, which is determined by culm diameter, culm wall thickness, and cell wall components, confers resistance to lodging (Ookawa et al., 2010; Wang et al., 2023). To date, research on lodging resistance has mainly focused on mutants with brittle culms, which can lead to many adverse phenotypes, making it difficult to use these mutants for rice production. Only a few genes associated with lodging resistance have been identified in natural germplasms. For example, *SCM2* (*APO1*), *SCM3* (*OsTB1*), and *OsCKX2* (*GN1a*) improve lodging resistance by increasing culm diameter and culm wall thickness (Ookawa et al., 2010; Yano et al., 2015; Cui et al., 2020; Tu et al., 2022). Therefore, it is important to dissect the genetic components of natural accessions and to explore related genes conferring lodging resistance.

We previously evaluated 795 rice accessions for lodging resistance traits, including culm diameter, culm wall thickness,

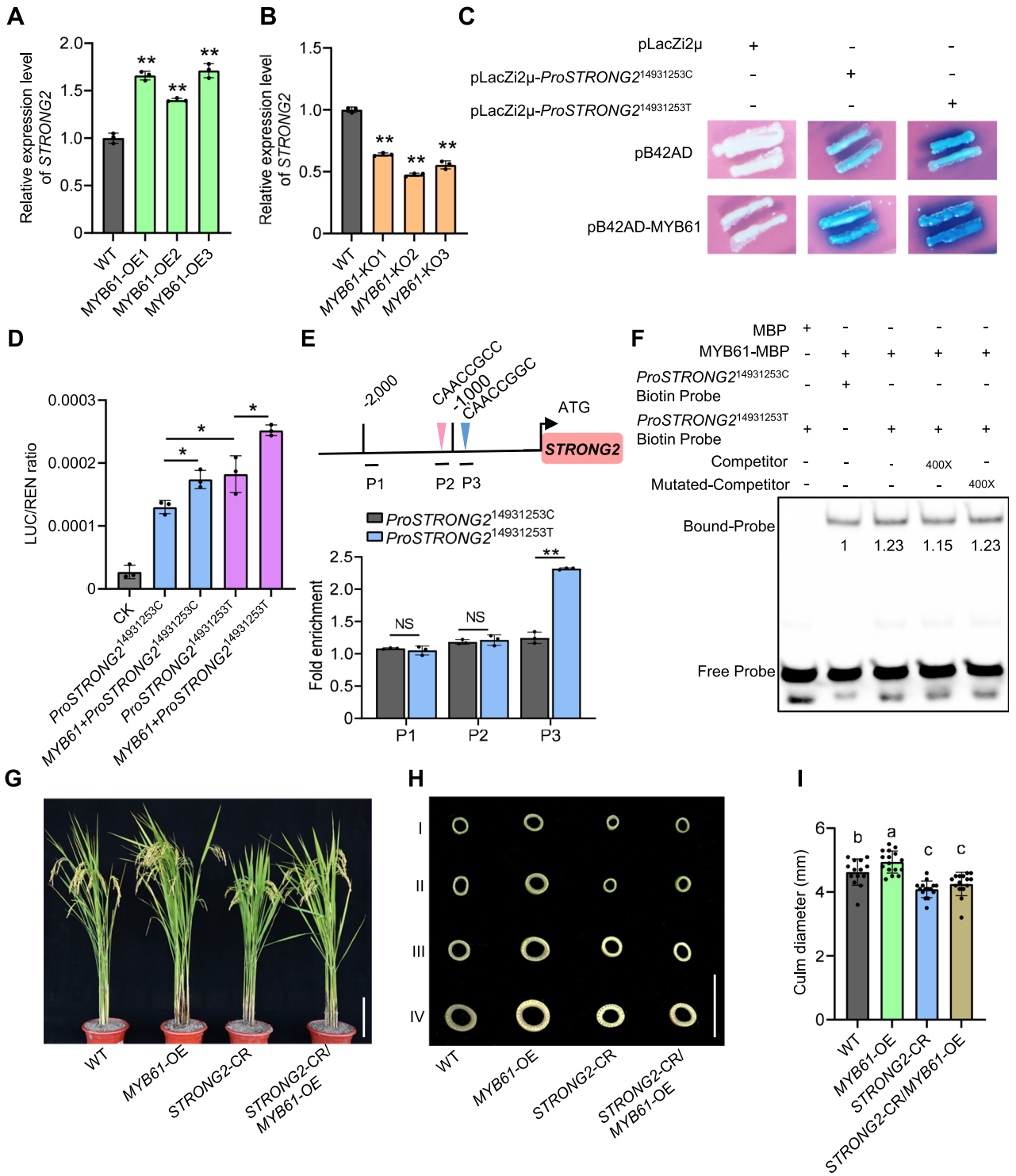

Figure 5. MYB61 activates *STRONG2* expression to regulate culm diameter

(A, B) Expression levels of *STRONG2* in the wild-type (WT) and *MYB61* overexpression transgenic lines **(A)** and knockout lines **(B)** were revealed by RT-qPCR. Values are means ± *SD* ($n = 3$). **(C)** Y1H assays show that MYB61 binds to both *ProSTRONG2*^{14931253C} and the *ProSTRONG2*^{14931253T} promoter. **(D)** Assays of the transcriptional activation of *ProSTRONG2*^{14931253C} and *ProSTRONG2*^{14931253T} activated by MYB61 in rice protoplasts. Values are mean ± *SD* ($n = 6$). **(E)** ChIP–qPCR assays for the differential binding affinity of MYB61 with *ProSTRONG2*^{14931253C} and the *ProSTRONG2*^{14931253T} promoter in *Pro35S:Flag-MYB61* protoplasts. Values are mean ± *SD* ($n = 3$). **(F)** Electrophoretic mobility shift assay shows that MYB61 binds to the *STRONG2* promoter *in vitro*. The mutant competitor probe contained a mutated binding motif. **(G, H)** Plant morphologies **(G)** and culm diameter **(H)** of the WT, *MYB61*-OE, *STRONG2*-CR and *STRONG2*-OE/*MYB61*-OE lines. Scale bar, 20 cm for **(E)**; scale bar, 1 cm for **(F)**. **(I)** Statistical results for culm diameter of the WT, *MYB61*-OE, *STRONG2*-CR and *STRONG2*-OE/*MYB61*-OE lines. $^*P < 0.05$; $^{**}P < 0.01$ as determined by two-tailed Student's *t*-test. In **(I),** different lowercase letters indicate a significant difference ($P < 0.05$) based on one-way ANOVA with the Duncan test.

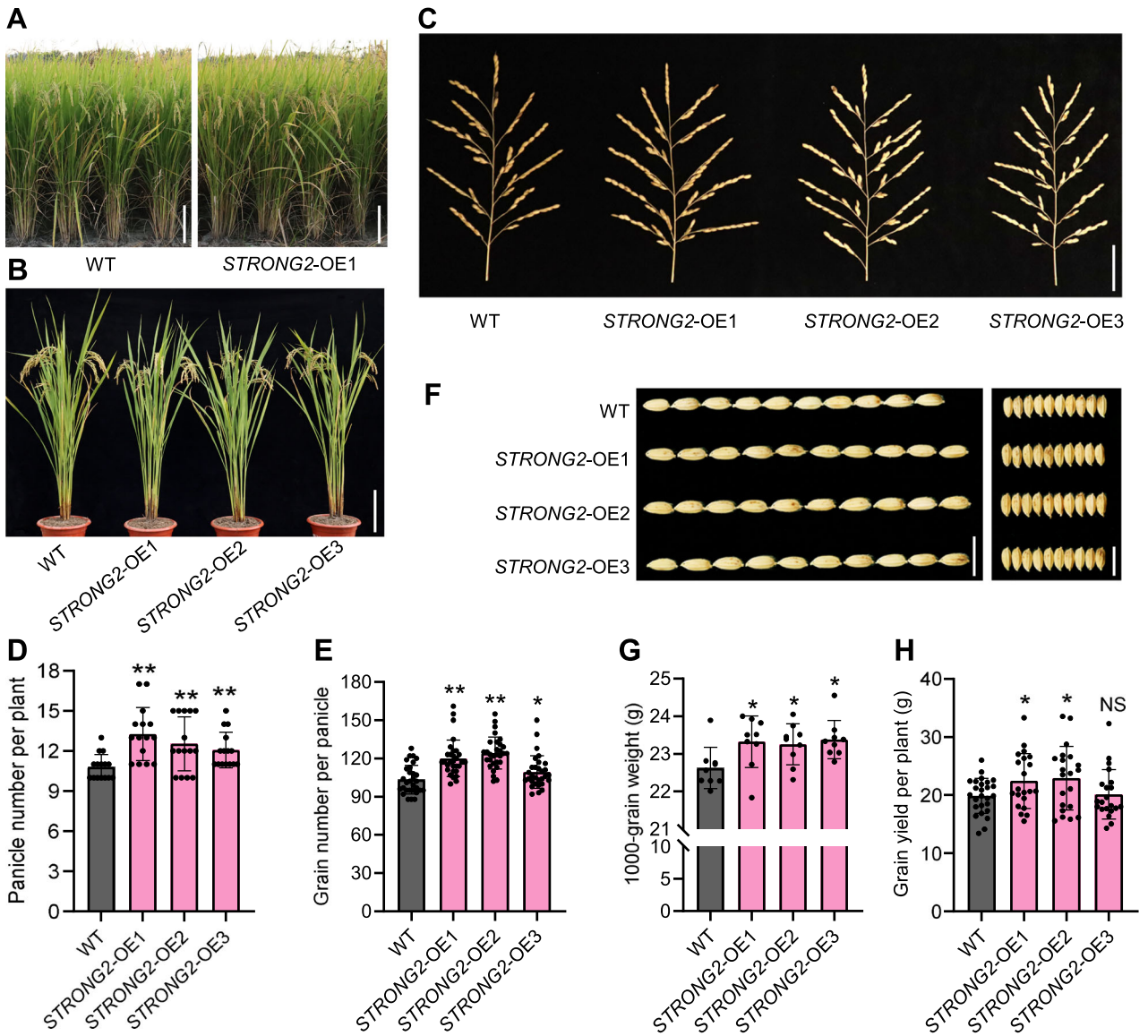

Figure 6. Overexpressing *STRONG2* enhances grain yield

(A, B) Phenotypes of the wild-type (WT) and *STRONG2* overexpressing lines grown in a field in Beijing, China, in 2023. Scale bars for **(A, B)**, 20 cm. **(C)** Panicles of the WT and *STRONG2* overexpressing lines. Scale bar, 5 cm. **(D, E)** Statistical analysis of panicle number per plant **(D)** and grain number per panicle **(E)** of WT and *STRONG2* overexpressing lines. Values are mean ± *SD* ($n > 15$). **(F)** Mature paddy grain of the WT and *STRONG2* overexpressing lines. Scale bars, 1 cm. **(G, H)** Statistical analysis of 1000-grain weight **(G)** and grain yield per plant **(H)** of the WT and *STRONG2* overexpressing lines. Values are mean ± *SD* ($n > 9$). $^{*}P < 0.05$; $^{**}P < 0.01$; NS, no significant difference as determined by two-tailed Student's *t*-test.

SM, BS, PR, and coefficient of lodging resistance (Rashid et al., 2022). We detected significant positive correlations among traits. In the current study, we conducted a GWAS using natural rice populations with different culm diameters and identified 10 QTLs on different chromosomes associated with this trait (Table S2). Among these, we discovered *STRONG2*, encoding a CSLA mannan synthase that positively regulates lodging resistance (Figure 1). Perhaps alleles of *STRONG2*, the first naturally occurring variants identified in *CSLA* genes, could be used to improve lodging resistance.

Numerous studies have revealed a negative trade-off between high yield and lodging resistance (Islam et al., 2007). Several breeding experiments have attempted to use alleles that confer strong stems, but these efforts have been unsuccessful due to the negative trade-off between culm strength and grain yield (Hirano et al., 2017). Therefore, it is important to comprehensively elucidate the genetic basis of culm strength and yield-related traits and to identify alleles that could be used to improve culm strength without negatively affecting grain yield. For example, *myb110* mutants show increased grain yield and lodging resistance (Wang et al., 2023). In this study, we demonstrated that *STRONG2* positively regulates lodging resistance and grain yield simultaneously in rice without affecting quality (Figures 1, 6, and S15), suggesting that this gene could be used in rice breeding efforts to increase lodging resistance.

Haplotype and genetic diversity analysis revealed that Hap1 is an inferior haplotype and is under positive selection (Figure 5; Table S4). Notably, Hap1 was primarily detected in the *tej* subpopulation, and the expression levels of *STRONG2* were lower in cultivars harboring Hap1 than in those with other haplotypes (Figure 4D). Why is Hap1 (*tej*) subject to positive selection? *japonica* rice has developed excellent low-temperature adaptability through long-term domestication and improvement, enabling survival in high-altitude or high-latitude regions (Zhang et al., 2017; Li et al., 2021; Lou et al., 2022). We noticed that the cultivars containing Hap1 are mainly present in high-altitude or high-latitude regions, indicating that this haplotype might also play an important role in the low-temperature response. These results suggest that Hap1 may confer improved cold resistance, favoring its selection. The possible pleiotropic effects of *STRONG2* should be further investigated.

The cell wall provides mechanical support for plant cells during growth, development, and adaptation to a constantly changing environment (Vaahtera et al., 2019). Cellulose and hemicellulose are important components of the cell wall that play crucial roles in plant growth and development, and protect cells from damage when subjected to various stresses. Mannans, which bind cellulose bundles to affect the mechanical properties of plant fibers, are a functionally diverse group of hemicellulosic polysaccharides (Voiniciuc, 2022). In some algae, mannan microfibers are even the main structural components of the cell wall. Mannan synthase, first identified from guar beans (*Cyamopsis tetragonoloba*), is a member of the CSLA family (Dhugga et al., 2004; Liepman et al., 2005). CSLAs synthesize mannan or glucomannan backbones *in vitro* (Liepman et al., 2005, 2007). CSLA2, CSLA7, and CSLA9 are responsible for glucomannan synthesis in Arabidopsis stems and embryos, which lack SCWs, indicating that mannan is involved in plant development (Goubet et al., 2009).

In the current study, we identified *STRONG2*, encoding the mannan synthase CSLA5, which regulates mannose and cellulose contents and affects SCW development in stems (Figure 3F–J). We suggest that, although the mannose content of the SCW is low, changes in its abundance affect the cellulose content of the SCW via a synergistic interaction. In addition, changes in cell wall components affect the integrity of the cell wall, perhaps influencing the response to relevant intercellular or intracellular signals and environmental signals that modulate plant growth and development (Du et al., 2022; Lin et al., 2022). We measured the expression levels of several genes associated with grain number and grain size in *STRONG2* knockout and overexpression lines, such as *NOG1*, *MADS17*, *RGN1*, *Gnp4*, *GNP6*, *CYCB2.1*, *CYCD7.1*, *EXPB3*, *EXPB7*, and *H1*. The expression levels of these genes underwent opposite changes in *STRONG2* knockout and overexpression lines (Figure S16), suggesting that the expression of these genes may have been altered due to changes in signaling. Taken together, our findings suggest that *STRONG2* may regulate grain number or grain size by affecting cell wall components, thus influencing grain development.

Previous studies have shown that MYB61 promotes SCW formation by influencing cellulose content, thereby enhancing lodging resistance (Gao et al., 2020). Our findings demonstrate that *STRONG2*, a target of MYB61, plays an important role in rice lodging by mediating the biosynthesis of cell wall compounds (Figure 7). Our identification of the MYB61-STRONG2 cascade provides further insight into the molecular mechanism of lodging resistance, suggesting strategies for breeding *japonica* rice varieties with improved yield.

MATERIALS AND METHODS

Plant materials and growth conditions

The 340 rice accessions used for GWAS and haplotype analysis were planted in Sanya (Hainan Province, China) under natural conditions. T_2 or later generations of transgenic plants were used for phenotypic evaluation, and they were planted in Beijing (China) during the summer season under natural paddy conditions. All the rice accessions used in this study are listed in Table S1.

GWAS

In total, 3,097,189 SNPs from 340 rice germplasms (including 141 *japonica* and 199 *indica*) with a quality control step (MAF $\geq$ 0.05 and missing rate <0.25) were retained for the GWAS using the CMLM model in the GAPIT package operated in the R environment (Tang et al., 2016). The population structure of PCA and kinship were taken into account as cofactors when performing GWASs using the CMLM model. The genome-wide LD decay of 340 rice germplasms was determined using PopLDdecay version 3.4 (Zhang et al., 2019) with parameters as follows: –maxdist 5000 –maf 0.05 –miss 0.25. The LD decay distance was determined as the LD decay to half of the maximum value. The genome-wide significance threshold was determined by permutation tests with 500 replications (Zhao et al., 2018). A region containing more than three consecutive significant SNPs and a distance between two SNPs less than the LD decay distance was considered a single significant associated signal (Guo et al., 2020). The SNP with the minimum *P*-value within the significant associated signal was considered to be the lead SNP. The interval of a single significant associated signal identified in this study was calculated as below: r^2 values were calculated between the lead SNP and all SNPs in its upstream and downstream 500 kb regions, and the interval was defined as a continue region where r^2 was more than 0.6 (Dong et al., 2016). For the analysis of candidate genes of the significantly associated signal, the continuous region containing SNPs closely linked with each other ($r^2 \geq 0.6$) was considered the local LD interval (Yano et al., 2016).

Vector constructions and plant transformation

To construct the CRISPR/Cas9 vector, a 20-bp PAM sequence from the *STRONG2* CDS was selected for specific recognition and cloned into the vector pHUE411 (Xing et al., 2014). To construct the *Pro35S:Flag-STRONG2* and *Pro35S:Flag-MYB61* vector, the full-length cDNA (without stop codons) of *STRONG2*

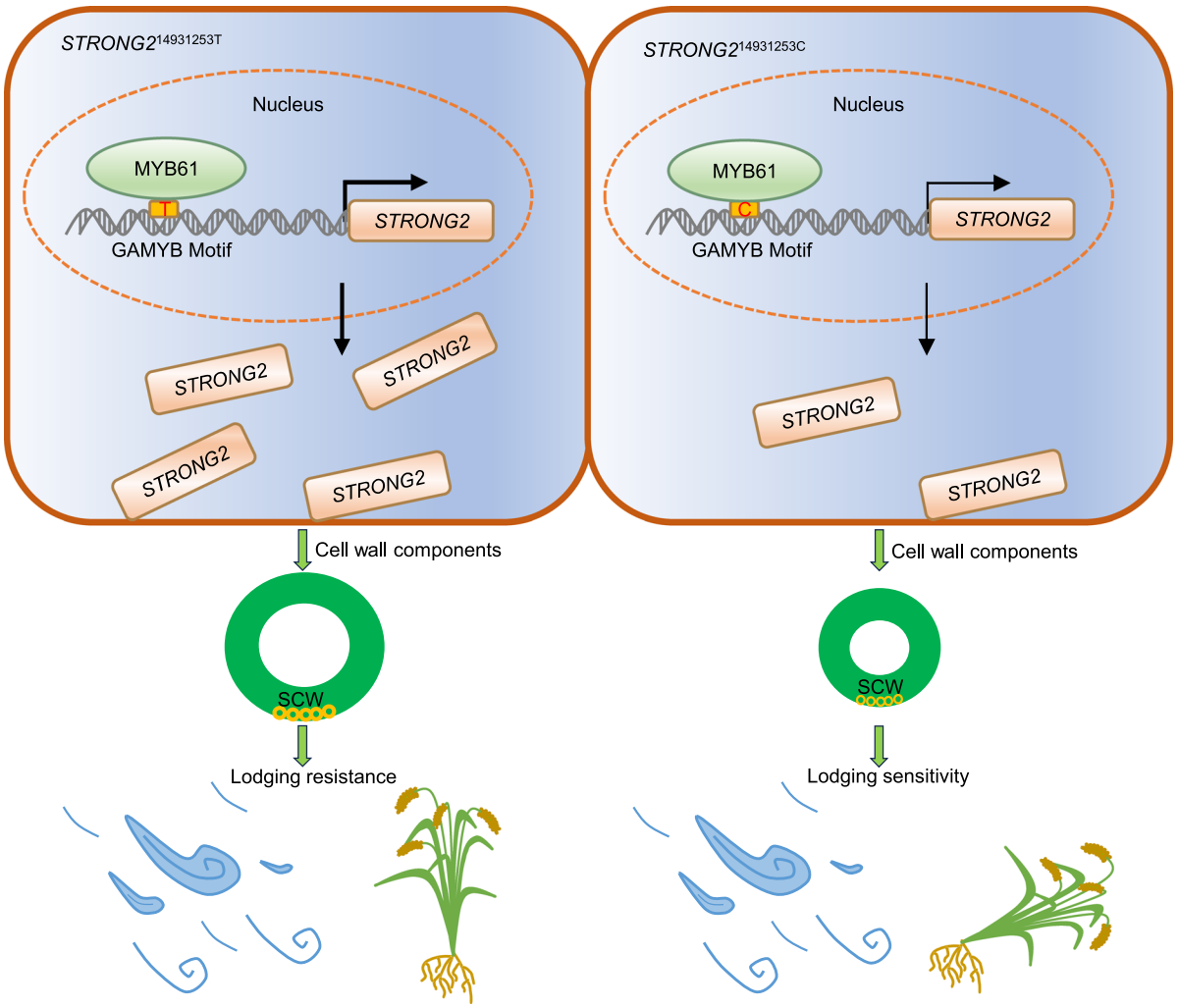

Figure 7. A working model of MYB61-STRONG2 module in regulating lodging resistance
MYB61 positively regulates the expression of *STRONG2*, ultimately affecting cell wall composition. The cell wall compositions affect secondary cell wall (SCW) formation. In *STRONG2*^{14931253T}, the SCW thickness was significantly increased because of the high expression of *STRONG2*, leading to enhanced lodging resistance. In *STRONG2*^{14931253C}, the expression of *STRONG2* is lower than *STRONG2*^{14931253T} and the SCW thickness was significantly decreased, leading to lodging sensitivity.

and *MYB61* were amplified and cloned into the binary plant expression vector pCM1307. For the construction of the GUS vector, 2,539 bp genomic fragments upstream of the ATG start codons from the *STRONG2* promoter were amplified and cloned into the binary plant expression vector pMDC162. For subcellular localization, the full-length cDNA of *STRONG2* without stop codon was amplified and cloned into the binary plant expression vector pSuper1300-GFP. For the complementary test, the native promoter sequence upstream of the start codon and the CDS were cloned into the binary vector pMDC163. To produce transgenic plants, these constructs were subsequently introduced into the corresponding rice cultivars via *Agrobacterium*-mediated transformation (Toki et al., 2006).

Phenotypic analysis

For the culm diameter and culm wall thickness measurement, the fourth internodes of the main stems were selected to measure the culm diameter and wall thickness using vernier caliper (MNT-150T, MNT) at the maturity stage of rice.

For the lodging resistance-related trait measurements, including PR, SM and BS, four main culms from different plants were measured at the mature stage. The bending load at breaking was measured at a distance of 4 cm between two supporting points using a testing machine (YYD-1, TOP Instrument, China), which was used to calculate the BS value. The SM was evaluated as previously reported (Ookawa et al., 2010). The measurement of the PR was performed at the 20 cm height and bending angle of 45° as previously reported (Kashiwagi and Ishimaru, 2004).

Scanning electron microscopy (SEM)

The fourth internode from development-matched WT and *STRONG2* transgenic lines were subjected to freehand-cut sectioning. The sections were then fixed in a 2.5%

glutaraldehyde solution (P1126, Solarbio, China). For SEM, the samples from internodes were sprayed with gold particles after dehydration through a gradient of ethanol and then observed with an S-3000N scanning electron microscope (Hitachi, Japan).

Histological analysis

The fourth internodes were sampled before heading and fixed in 50% FAA solution. The samples were embedded in Paraplast, stained with toluidine blue, and photographed under an IX71 microscope (Olympus, Japan). Cell size and sclerenchyma tissue thickness were measured using ImageJ software.

Cell wall composition analysis

The mature fourth internodes collected from the WT and *STRONG2* transgenic lines were dried and ball milled into fine powders. Residues were prepared and hydrolyzed in 2 M trifluoroacetic acid and then treated in Updegraff reagent. The cellulose content was measured by the anthrone method (Updegraff, 1969). The lignin content was measured using the acetyl bromide method (Huang et al., 2015). The mannose contents were detected using the GC-MS method by MetWare (http://www.metware.cn/) based on the Agilent 8890-5977B platform.

Expression pattern analysis

RT-qPCR was used to check the expression levels of *STRONG2* and the other genes involved in this study. Total RNA was extracted from fresh tissues using a plant RNA isolation kit following the manufacturer's instructions (RN0302, Aidlab, China). cDNA was synthesized using the TRUEscript First Strand cDNA Synthesis Kit (PC5802, Aidlab, China). RT-qPCR was conducted using SYBR® Premix Ex Taq II (RR820A, TaKaRa, Japan) on an ABI 7500 real-time PCR system (Applied Biosystems, Foster City, CA, USA). Rice *ubiqutin1* (LOC_Os03g13170) was used as an internal control.

GUS staining was conducted to analyze the expression pattern of *STRONG2*. Tissues from transgenic plants harboring the *ProSTRONG2:GUS* reporter were obtained and infiltrated in GUS staining solution as previously reported (Zhang et al., 2018). The stems were observed under a BX60 microscope (Olympus, Japan).

Subcellular localization

ProSuper1300:STRONG2-GFP constructs were expressed transiently in rice protoplasts and tobacco to determine the subcellular location. Fluorescence signals were observed by confocal laser scanning FV1000 microscopy (Olympus, Japan) after culture for 18 h at 28°C (Excitation spectrum: 488 nm; Emission spectrum: 510 nm).

Protein sequence and phylogenetic analysis

Arabidopsis thaliana of STRONG2 protein sequence was obtained from the TAIR (http://www.arabidopsis.org/index.jsp). The sequences of other STRONG2 protein homologs were acquired by searching the database from NCBI (https://www.ncbi.nlm.nih.gov/). Multiple sequence alignments were conducted by ClustalX. The phylogenetic tree was constructed using the maximum likelihood method by MEGA 5.0 with 1,000 bootstrap replicates (Tamura et al., 2011).

Dual-luciferase assays

The promoter sequence of *STRONG2* was amplified and then cloned into the pGreenII-0800-Luc vector, which was used as a reporter. The full-length cDNA of *MYB61* was cloned into the pGreenII 62-SK vector, which was used as an effector. Reporters and effectors were subsequently transformed into rice protoplasts. The luciferase (LUC) and Renilla luciferase (REN) activities were measured using the Dual-Luciferase® Reporter Assay System (E1910, Promega, Madison City, Wisconsin, USA) using a GloMax® Discover Microplate Reader (Promega).

Yeast one-hybrid assays

The full-length cDNA of *MYB61* was cloned into the pB42AD vector. Genomic fragments of the *STRONG2* promoter region starting at 2,539 kb upstream of the ATG start codon were amplified and cloned into the pLacZi2μ vector as reporters. *MYB61-pB42AD* and co-transformed with the reporter or control (empty pLacZi2μ vector) into the yeast strain *EGY48* through the PEG/LiAc-mediated method. Positive clones were cultured on SD/−Ura−Trp plates containing β-D-galactopyranoside to check for possible interactions between MYB61 and the reporter.

ChIP–qPCR analysis

Rice protoplasts from the *Pro35S:Flag-MYB61* transgenic plants were used for ChIP–qPCR. ChIP assays were performed following the manufacturer's instructions, with minor modifications (Weng et al., 2018; Gao et al., 2020). The products from the ChIP assays were used for RT-qPCR, which was performed three times for each sample, and the expression levels were normalized to the input sample for enrichment detection.

Electrophoretic mobility shift assays

The cDNA of *MYB61* was amplified and cloned into the vector pMAL-c5X to construct the MBP-MYB61 vector. The recombinant MBP-MYB61 constructs and MBP were introduced into *Escherichia coli* Rosetta (DE3) cells and purified following a PurKine™ MBP-Tag Protein Purification Kit (KTP2020, Abbkine, China). The probe was selected from the *STRONG2* promoter region (919–948 bp upstream of the ATG codon), which contains a GAMYB motif (CAACC**G**GC). The mutant probe was synthesized by replacing CAACC**G**GC with TTTTTTTT. The biotin-labeled and unlabeled probes were synthesized and purified as forward/reverse primers by the Beijing Genomics Institute (BGI). EMSA reaction was performed using a Light Shift Chemiluminescent EMSA kit (20148, Thermos, Germany) as described. Signals were detected using a ChemiScope6100 Chemiluminescent Imaging System (Clinx, China).

Haplotype, phylogenetic and nucleotide diversity analyses

DNA sequences of SNPs in *STRONG2* from 340 cultivated accessions were obtained from the 3000 Rice Genome

Project. Twenty-three SNPs were used to perform haplotype analysis. The re-sequenced data of 701 rice accessions, including 558 cultivated rice accessions and 143 common wild rice accessions that were obtained from the 3000 Rice Genome Project and a previous publication (Huang et al., 2012; Wang et al., 2018), were used for phylogenetic tree analysis and nucleotide diversity analysis. The neighbor-joining phylogenetic tree was constructed using MEGA 5.0 with 1,000 replications of bootstrap tests. Then the result was visualized and annotated using EvolView (Zhang et al., 2012). Dnasp5.0 was used to define the haplotypes, and Arlequin version 3.5 was used to calculate the distance between different haplotypes (Librado and Rozas, 2009; Excoffier and Lischer, 2010). The minimum spanning tree was constructed using Hapstar-0.6 and then visualized by artificial modification (Teacher and Griffiths, 2011).

For nucleotide diversity (π), the coding region and 20 kb upstream and downstream flanking sequences of *STRONG2* in wild rice, *tej*, *trj* and *ind* were calculated using VCFtools. Tajima's *D* was calculated and performed using DnaSP 5.10 (Librado and Rozas, 2009).

Primers

The relevant primers used are listed in Table S6.

ACKNOWLEDGEMENTS

This work was funded by the Biological Breeding-National Science and Technology Major Project (2023ZD0406803), the AgroST Project (NK2022050103), the National Natural Science Foundation of China (32272123 and 32072036), the Hainan Provincial Natural Science Foundation of China (324QN358), the Chinese Universities Scientific Fund (2024TC189), the Postdoctoral Research Projects in Hainan Province (343812), the Hainan Seed Industry Laboratory and the China National Seed Group (B23YQ1517 and B23CQ15HP), the Special Plan for Key Laboratory of "Western Light Western cross team" (xbzg-zdsys-202111), and the 2115 Talent Development Program of China Agricultural University.

CONFLICTS OF INTEREST

The authors declare no conflict of interest.

AUTHOR CONTRIBUTIONS

Z.Z., Z.L., C.C., and Y.Z. designed the research and revised the manuscript. Y.Z., and J.G. performed most of the experiments. Y.Z. and X.W. analyzed the data. R.R., H.W., and Q.H. performed partial experiments. Y.Z. wrote the manuscript. X.S., J.L., H.Z., P.X. and Q.Q. provided technical assistance. All authors have read and agreed to the published version of the manuscript.

Edited by: Letian Chen, South China Agricultural University, China

Received Sep. 13, 2024; **Accepted** Dec. 9, 2024; **Published** Jan. 6, 2025

REFERENCES

Burton, R.A., Wilson, S.M., Hrmova, M., Harvey, A.J., Shirley, N.J., Medhurst, A., Stone, B.A., Newbigin, E.J., Bacic, A., Fincher, G.B., et al. (2006). Cellulose synthase-like *CslF* genes mediate the synthesis of cell wall (1,3;1,4)-β-D-glucans. Science **311:** 1940–1942.

Cocuron, J.C., Lerouxel, O., Drakakaki, G., Alonso, A.P., Liepman, A.H., Keegstra, K., Raikhel, N., and Wilkerson, C.G. (2007). A gene from the cellulose synthase-like C family encodes a beta-1,4 glucan synthase. Proc. Natl. Acad. Sci. U.S.A. **104:** 8550–8555.

Cui, Y., Hu, X., Liang, G., Feng, A., Wang, F., Ruan, S., Dong, G., Shen, L., Zhang, B., Chen, D., et al. (2020). Production of novel beneficial alleles of a rice yield-related QTL by CRISPR/Cas9. Plant. Biotechnol. J. **18:** 1987–1989.

Dhugga, K.S., Barreiro, R., Whitten, B., Stecca, K., Hazebroek, J., Randhawa, G.S., Dolan, M., Kinney, A.J., Tomes, D., Nichols, S. et al. (2004). Guar seed beta mannan synthase is a member of the cellulose synthase super gene family. Science **303:** 363–366.

Ding, Z., Lin, Z., Li, Q., Wu, H., Xiang, C., and Wang, J. (2015). *DNL1*, encodes cellulose synthase-like D4, is a major QTL for plant height and leaf width in rice (*Oryza sativa* L.). Biochem. Biophys. Res. Commun. **457:** 133–140.

Doblin, M.S., Pettolino, F.A., Wilson, S.M., Campbell, R., Burton, R.A., Fincher, G.B., Newbigin, E., and Bacic, A. (2009). A barley cellulose synthase-like *CSLH* gene mediates (1,3;1,4)-beta-d-glucan synthesis in transgenic Arabidopsis. Proc. Natl. Acad. Sci. U.S.A. **106:** 5996–6001.

Dong, H., Zhao, H., Xie, W., Han, Z., Li, G., Yao, W., Bai, X., Hu, Y., Guo, Z., Lu, K., et al. (2016). A novel Tiller angle gene, *TAC3*, together with *TAC1* and *D2* largely determine the natural variation of Tiller angle in rice cultivars. PLoS. Genet. **12:** e1006412.

Du, J., Anderson, C., and Xiao, C. (2022). Dynamics of pectic homogalacturonan in cellular morphogenesis and adhesion, wall integrity sensing and plant development. Nat. Plants **8:** 332–340.

Excoffier, L., and Lischer, H.E. (2010). Arlequin suite ver 3.5: A new series of programs to perform population genetics analyses under Linux and Windows. Mol. Ecol. Resour. **10:** 564–567.

Gao, Y., Xu, Z., Zhang, L., Li, S., Wang, S., Yang, H., Liu, X., Zeng, D., Liu, Q., Qian, Q., et al. (2020). MYB61 is regulated by GRF4 and promotes nitrogen utilization and biomass production in rice. Nat. Commun. **11:** 5219.

Goubet, F., Barton, C.J., Mortimer, J.C., Yu, X.L., Zhang, Z.N., Miles, G.P., Richens, J., Liepman, A.H., Seffen, K., and Dupree, P. (2009). Cell wall glucomannan in Arabidopsis is synthesised by CSLA glycosyltransferases, and influences the progression of embryogenesis. Plant J. **60:** 527–538.

Guo, H., Zeng, Y., Li, J., Ma, X., Zhang, Z., Lou, Q., Li, J., Gu, Y., Zhang, H., Li, J., et al. (2020). Differentiation, evolution and utilization of natural alleles for cold adaptability at the reproductive stage in rice. Plant. Biotechnol. J. **18:** 2491–2503.

Handford, M.G., Baldwin, T.C., Goubet, F., Prime, T.A., Miles, J., Yu, X., and Dupree, P. (2003). Localisation and characterisation of cell wall mannan polysaccharides in *Arabidopsis thaliana*. Planta **218:** 27–36.

Hirano, K., Ordonio, R.L., and Matsuoka, M. (2017). Engineering the lodging resistance mechanism of post-Green revolution rice to meet future demands. Proc. Jpn. Acad. Ser. B Phys. Biol. Sci. **93:** 220–233.

Hu, J., Zhu, L., Zeng, D., Gao, Z., Guo, L., Fang, Y., Zhang, G., Dong, G., Yan, M., Liu, J., et al. (2010). Identification and characterization of

NARROW AND ROLLED LEAF 1, a novel gene regulating leaf morphology and plant architecture in rice. Plant Mol. Biol. **73:** 283–292.

Huang, D., Wang, S., Zhang, B., Shang-Guan, K., Shi, Y., Zhang, D., Liu, X., Wu, K., Xu, Z., Fu, X., et al. (2015). A gibberellin-mediated DELLA-NAC signaling cascade regulates cellulose synthesis in rice. Plant Cell **27:** 1681–1696.

Huang, X., Kurata, N., Wei, X., Wang, Z.X., Wang, A., Zhao, Q., Zhao, Y., Liu, K., Lu, H., Li, W., et al. (2012). A map of rice genome variation reveals the origin of cultivated rice. Nature **490:** 497–501.

Islam, M.S., Peng, S., Visperas, R.M., Ereful, N., Bhuiya, M.S.U., and Julfiquar, A.W. (2007). Lodging-related morphological traits of hybrid rice in a tropical irrigated ecosystem. Field Crop. Res. **101:** 240–248.

Kashiwagi, T., and Ishimaru, K. (2004). Identification and functional analysis of a locus for improvement of lodging resistance in rice. Plant Physiol. **134:** 676–683.

Kashiwagi, T., Madoka, Y., Hirotsu, N., and Ishimaru, K. (2006). Locus *prl5* improves lodging resistance of rice by delaying senescence and increasing carbohydrate reaccumulation. Plant Physiol. Biochem. **44:** 152–157.

Kaur, S., Dhugga, K.S., Beech, R., and Singh, J. (2017). Genome-wide analysis of the *cellulose synthase-like (Csl)* gene family in bread wheat (*Triticum aestivum* L.). BMC Plant Biol. **17:** 193.

Kim, C.M., Park, S.H., Je, B.I., Park, S.H., Park, S.J., Piao, H.L., Eun, M.Y., Dolan, L. and Han, C.D. (2007). *OsCSLD1*, a cellulose synthase-like D1 gene, is required for root hair morphogenesis in rice. Plant Physiol. **143:** 1220–1230.

Kumar, M., Campbell, L., and Turner, S. (2016). Secondary cell walls: Biosynthesis and manipulation. J. Exp. Bot. **67:** 515–531.

Li, F., Zhang, M., Guo, K., Hu, Z., Zhang, R., Feng, Y., Yi, X., Zou, W., Wang, L., Wu, C., et al. (2015). High level hemicellulosic arabinose predominately affects lignocellulose crystallinity for genetically enhancing both plant lodging resistance and biomass enzymatic digestibility in rice mutants. Plant Biotech. J. **13:** 514–525.

Li, J., Zeng, Y., Pan, Y., Zhou, L., Zhang, Z., Guo, H., Lou, Q., Shui, G., Huang, H., Tian, H., et al. (2021). Stepwise selection of natural variations at *CTB2* and *CTB4a* improves cold adaptation during domestication of japonica rice. New Phytol. **231:** 1056–1072.

Li, M., Xiong, G., Li, R., Cui, J., Tang, D., Zhang, B., Pauly, M., Cheng, Z., and Zhou, Y. (2009). Rice cellulose synthase-like D4 is essential for normal cell-wall biosynthesis and plant growth. Plant J. **60:** 1055–1069.

Librado, P., and Rozas, J. (2009). DnaSP v5: A software for comprehensive analysis of DNA polymorphism data. Bioinformatics **25:** 1451–1452.

Liepman, A.H., Nairn, J., Willats, W.G.T., Sørenson, I., Roberts, A.W., and Keegstra, K. (2007). Functional genomic analysis supports conservation of function among cellulose synthase-like a gene family members and suggests diverse roles of mannans in plants. Plant Physiol. **143:** 1881–1893.

Liepman, A.H., Wilkerson, C.G., and Keegstra, K. (2005). Expression of cellulose synthase-like (Csl) genes in insect cells reveals that CslA family members encode mannan synthases. Proc. Natl. Acad. Sci. U.S.A. **102:** 2221–2226.

Lin, W., Tang, W., Pan, X., Huang, A., Gao, X., Anderson, C.T., and Yang, Z. (2022). Arabidopsis pavement cell morphogenesis requires FERONIA binding to pectin for activation of ROP GTPase signaling. Curr. Biol. **32:** 497–507.

Little, A., Lahnstein, J., Jeffery, D.W., Khor, S.F., Schwerdt, J.G., Shirley, N.J., Hooi, M., Xing, X., Burton, R.A., and Bulone, V. (2019). A novel (1,4)-β-linked glucoxylan is synthesized by members of the cellulose synthase-like F gene family in land plants. ACS Cent. Sci. **5:** 73–84.

Lou, Q., Guo, H., Li, J., Han, S., Khan, N.U., Gu, Y., Zhao, W., Zhang, Z., Zhang, H., Li, Z., et al. (2022). Cold-adaptive evolution at the reproductive stage in Geng/japonica subspecies reveals the role of *OsMAPK3* and *OsLEA9*. Plant J. **111:** 1032–1051.

Okuno, A., Hirano, K., Asano, K., Takase, W., Masuda, R., Morinaka, Y., Ueguchitanaka, M., Kitano, H., and Matsuoka, M. (2014). New approach to increasing rice lodging resistance and biomass yield through the use of high gibberellin producing varieties. PLoS One **9:** e86870.

Ookawa, T., Hobo, T., Yano, M., Murata, K., Ando, T., Miura, H., Asano, K., Ochiai, Y., Ikeda, M., Nishitani, R., et al. (2010). New approach for rice improvement using a pleiotropic QTL gene for lodging resistance and yield. Nat. Commun. **1:** 132.

Peng, X., Pang, H., Abbas, M., Yan, X., Dai, X., Li, Y., and Li, Q. (2019). Characterization of *Cellulose synthase-like D* (*CSLD*) family revealed the involvement of *PtrCslD5* in root hair formation in *Populus trichocarpa*. Sci. Rep. **9:** 1452.

Rashid, M.A.R., Zhao, Y., Azeem, F., Zhao, Y., Ahmed, H.G.M., Atif, R.M., Pan, Y., Zhu, X., Liang, Y., Zhang, H., et al. (2022). Unveiling the genetic architecture for lodging resistance in rice (*Oryza sativa. L*) by genome-wide association analyses. Front. Genet. **13:** 960007.

Scheller, H.V., and Ulvskov, P. (2010). Hemicelluloses. Annu. Rev. Plant Biol. **61:** 263–289.

Tamura, K., Peterson, D., Peterson, N., Stecher, G., Nei, M., and Kumar, S. (2011). MEGA5: molecular evolutionary genetics analysis using maximum likelihood, evolutionary distance, and maximum parsimony methods. Mol. Biol. Evol. **28:** 2731–2739.

Tang, Y., Liu, X., Wang, J., Li, M., Wang, Q., Tian, F., Su, Z., Pan, Y., Liu, D., Lipka, A.E., et al. (2016). GAPIT Version 2: An enhanced integrated tool for genomic association and prediction. Plant Genome **9:** 1–9.

Taylor-Teeples, M., Lin, L., de Lucas, M., Turco, G., Toal, T.W., Gaudinier, A., Young, N.F., Trabucco, G.M., Veling, M.T., Lamothe, R., et al. (2015). An *Arabidopsis* gene regulatory network for secondary cell wall synthesis. Nature **517:** 571–575.

Teacher, A.G.F., and Griffiths, D.J. (2011). HapStar: Automated haplotype network layout and visualization. Mol. Ecol. Resour. **11:** 151–153.

Toki, S., Hara, N., Ono, K., Onodera, H., Tagiri, A., Oka, S., and Tanaka, H. (2006). Early infection of scutellum tissue with *Agrobacterium* allows high-speed transformation of rice. Plant J. **47:** 969–976.

Tu, B., Tao, Z., Wang, S., Zhou, L., Zheng, L., Zhang, C., Li, X., Zhang, X., Yin, J., Zhu, X., et al. (2022). Loss of *Gn1a*/*OsCKX2* confers heavy-panicle rice with excellent lodging resistance. J. Integr. Plant Biol. **64:** 23–38.

Updegraff, D.M. (1969). Semimicro determination of cellulose in biological materials. Anal. Biochem. **32:** 420–424.

Vaahtera, L., Schulz, J., and Hamann, T. (2019). Cell wall integrity maintenance during plant development and interaction with the environment. Nat. Plants **5:** 924–932.

Vega-Sánchez, M.E., Verhertbruggen, Y., Christensen, U., Chen, X., Sharma, V., Varanasi, P., Jobling, S.A., Talbot, M., White, R.G., Joo, M., et al. (2012). Loss of *Cellulose synthase-like F6* function affects mixed-linkage glucan deposition, cell wall mechanical properties, and defense responses in vegetative tissues of rice. Plant Physiol. **159:** 56–69.

Voiniciuc, C. (2022). Modern mannan: A hemicellulose's journey. New Phytol. **234:** 1175–1184.

Wang, T., Jin, Y., Deng, L., Li, F., Wang, Z., Zhu, Y., Wu, Y., Qu, H., Zhang, S., Liu, Y., et al. (2023). The transcription factor MYB110 regulates plant height, lodging resistance, and grain yield in rice. Plant Cell **36:** 298–323.

Wang, W., Mauleon, R., Hu, Z., Chebotarov, D., Tai, S., Wu, Z., Li, M., Zheng, T., Fuentes, R.R., Zhang, F., et al. (2018). Genomic variation in 3,010 diverse accessions of Asian cultivated rice. Nature **557:** 43–49.

Weng, X., Zhou, S., Zong, W., and Ouyang, Y.D. (2018). ChIP assay in rice. Bio-Protocol **101:** e1010135

Xing, H., Dong, L., Wang, Z., Zhang, H., Han, C., Liu, B., Wang, X., and Chen, Q. (2014). A CRISPR/Cas9 toolkit for multiplex genome editing in plants. BMC Plant Biol. **14:** 327.

Yang, J., Bak, G., Burgin, T., Barnes, W.J., Mayes, H.B., Peña, M.J., Urbanowicz, B.R., and Nielsen, E. (2020). Biochemical and genetic analysis identify CSLD3 as a beta-1,4-glucan synthase that functions during plant cell wall synthesis. Plant Cell **32:** 1749–1767.

Yano, K., Ookawa, T., Aya, K., Ochiai, Y., Hirasawa, T., Ebitani, T., Takarada, T., Yano, M., Yamamoto, T., Fukuoka, S., et al. (2015). Isolation of a novel lodging resistance QTL gene involved in strigolactone signaling and its pyramiding with a QTL gene involved in another mechanism. Mol. Plant **8:** 303–314.

Yano, K., Yamamoto, E., Aya, K., Takeuchi, H., Lo, P., Hu, L., Yamasaki, M., Yoshida, S., Kitano, H., Hirano, K., et al. (2016). Genome-wide association study using whole-genome sequencing rapidly identifies new genes influencing agronomic traits in rice. Nat. Genet. **48:** 927–934.

Yin, Y., Johns, M.A., Cao, H., and Rupani, M. (2014). A survey of plant and algal genomes and transcriptomes reveals new insights into the evolution and function of the cellulose synthase superfamily. BMC Genomics **15:** 260.

Yoshikawa, T., Eiguchi, M., Hibara, K.I., Ito, J.I., and Nagato, Y. (2013). Rice *SLENDER LEAF 1* gene encodes cellulose synthase-like D4 and is specifically expressed in M-phase cells to regulate cell proliferation. J. Exp. Bot. **64:** 2049–2061.

Zhang, C., Dong, S., Xu, J., He, W., and Yang, T. (2019). PopLDdecay: A fast and effective tool for linkage disequilibrium decay analysis based on variant call format files. Bioinformatics **35:** 1786–1788.

Zhang, H., Gao, S., Lercher, M.J., Hu, S., and Chen, W. (2012). EvolView, an online tool for visualizing, annotating and managing phylogenetic trees. Nucleic Acids Res. **40:** W569–W572.

Zhang, S., Hu, H., Cui, S., Yan, L., Wu, B., and Wei, S. (2023). Genome-wide identification and functional analysis of the cellulose synthase-like gene superfamily in common oat (*Avena sativa* L.). Phytochemistry **218:** 113940.

Zhang, Z., Li, J., Pan, Y., Li, J., Zhou, L., Shi, H., Zeng, Y., Guo, H., Yang, S., Zheng, W., et al. (2017). Natural variation in *CTB4a* enhances rice adaptation to cold habitats. Nat. Commun. **8:** 14788.

Zhang, Z., Li, J., Tang, Z., Sun, X., Zhang, H., Yu, J., Yao, G., Li, G., Guo, H., Li, J., et al. (2018). Gnp4/LAX2, a RAWUL protein, interferes with the OsIAA3-OsARF25 interaction to regulate grain length via the auxin signaling pathway in rice. J. Exp. Bot. **69:** 4723–4737.

Zhao, H., Li, Z., Wang, Y., Wang, J., Xiao, M., Liu, H., Quan, R., Zhang, H., Huang, R., Zhu, L., et al. (2022). Cellulose synthase-like protein OsCSLD4 plays an important role in the response of rice to salt stress by mediating abscisic acid biosynthesis to regulate osmotic stress tolerance. Plant. Biotechnol. J. **20:** 468–484.

Zhao, Y., Zhang, H., Xu, J., Jiang, C., Yin, Z., Xiong, H., Xie, J., Wang, X., Zhu, X., Li, Y., et al. (2018). Loci and natural alleles underlying robust roots and adaptive domestication of upland ecotype rice in aerobic conditions. PLoS. Genet. **14:** e1007521.

Zou, X., Zhen, Z., Ge, Q., Fan, S., Liu, A., Gong, W., Li, J., Gong, W., Shi, Y., Fan, L., et al. (2017). Genome-wide identification and analysis of the evolution and expression patterns of the cellulose synthase gene superfamily in *Gossypium* species. Gene **646:** 28–38.

SUPPORTING INFORMATION

Additional Supporting Information may be found online in the supporting information tab for this article: http://onlinelibrary.wiley.com/doi/10.1111/jipb.13830/suppinfo

Figure S1. Population structure and culm diameter phenotypic variation in the association populations
Figure S2. Linkage disequilibrium (LD) decay of the association populations
Figure S3. Quantile–quantile plots of observed versus expected $-Log_{10}(P)$ values of GWAS for culm diameter
Figure S4. Genome-wide threshold for GWAS based on permutation tests
Figure S5. Expression level of seven potential candidate genes for *qOD3.2* in the stem
Figure S6. Phylogenetic analysis of *STRONG2*
Figure S7. Culm morphology comparison between WT and *STRONG2* knockout transgenic lines
Figure S8. Comparison of culm morphology between WT and *STRONG2* overexpressing lines
Figure S9. The relationship between STRONG2 and CESAs
Figure S10. Comparison of culm morphology between YF and IL103
Figure S11. Haplotype network of *STRONG2*
Figure S12. *MYB61* positively regulates culm diameter
Figure S13. Phenotypes of the WT and *STRONG2* overexpressing lines
Figure S14. Phenotypes of the WT and *STRONG2* knockout lines
Figure S15. Grain chalkiness of the WT and *STRONG2* transgenic lines
Figure S16. *STRONG2* modulates the expression of grain-number- and grain-size-related genes
Table S1. Information on *Oryza sativa* L. varieties and wild rice
Table S2. Summary of the significant SNPs detected by GWAS
Table S3. Candidate genes of *STRONG2* in *qOD3.2*
Table S4. Average nucleotide diversity and Tajimas'*D* of *STRONG2* and the 20 kb flanking region
Table S5. The *cis*-acting elements in the *STRONG2* promoter
Table S6. Primers used in this study